Journal of
Nanoscience and Nanotechnology
Vol. 10, 4663–4666, 2010

Co Nanoislands on Au(111) and Cu(111) Surfaces Studied by Scanning Tunneling Microscopy and Spectroscopy

H. W. Chang[1,*], B. F. Wu[1], Y. D. Yao[2], W. B. Su[3], and C. S. Chang[3]

[1] *Department of Physics, Tunghai University, Taichung, 407 Taiwan*
[2] *Department of Materials Engineering, Tatung University, Taipei, 104 Taiwan*
[3] *Institute of Physics, Academia Sinica, Taipei, 115 Taiwan*

Co nanoislands on the Au(111) and Cu(111) surfaces have been studied by scanning tunneling microscopy and spectroscopy. The experimental results showed that Co nanoislands prefer to aggregate at the step edge and dislocation sites on the reconstructed Au(111) surface and at the step edge on the Cu(111) surface, respectively. In addition, based on *dZ/dV–V* spectra, in both the Co/Au(111) and the Co/Cu(111) systems, Gundlach oscillation was observed. From the peak shift of *dZ/dV–V* spectra between Co nanoisland and substrate surface, we can quantitatively obtain that the constant energy separation is -0.13 ± 0.01 eV for the Co/Au(111) system, and 0.41 ± 0.02 eV for the Co/Cu(111) system, respectively. These values indicate the work function difference between Co nanoisland and these surfaces.

Keywords: Magnetic Film, Scanning Tunneling Microscopy.

1. INTRODUCTION

Since Co/Au/Co and Co/Cu/Co sandwich structures with perpendicular magnetic anisotropy (PMA) and large magnetoresistance (MR) ratio were discovered by Chappert and Parkin, respectively, Co/Au and Co/Cu multilayers have drawn much attention due to their attractive physical properties and potential applications in the magnetic recording media.[1–8] However, their magnetic performances depend strongly on the interface morphology, and therefore, a great deal of related work has been done on the study of the Co/Au and Co/Cu interfaces.[9–18]

In a Co/Au(111) system, the large lattice mismatch of 14% between Co and Au induces the characteristic growth mode of Co films. Scanning tunneling microscopy (STM) study has shown that Co deposited at room temperature starts to nucleate at a kink of the reconstructed Au(111) surface with a zigzag, forming islands with a hexagonal closed-packed (hcp) structure, and then these islands become coalesced and connected to one another to form a film domain.[11] In addition, ferromagnetism with perpendicular anisotropy is observed when the thickness of a Co layer evaporated on the reconstructed Au(111) surface at room temperature is larger than 1.6 monolayers (ML).[12–13] On the other hand, in a Co/Cu system, because of the small lattice mismatch of 1.9% and the low miscibility of Co in bulk Cu, Co/Cu is considered as a heteroepitaxial system with a high degree of perfection. While this has been verified for the layer-by-layer growth of Co on a Cu(100) surface for a thickness above 2 ML, it has not been verified for Co on a Cu(111) surface.[14–17] Furthermore, Co grows initially on Cu(111) substrate in the form of bilayer islands in the shape of triangles that are rotated 180° with respect to each other. It has been observed by Spin-Polarized STM that these two types of Co islands exhibit perpendicular magnetic anisotropy with large coercivity of 1–1.5 T and M_r/M_s of nearly 1.[18] Accordingly, these two systems have a promising future in next-generation magnetic storage.

However, little information about electronic properties, especially for work function, of Co nanoislands on the reconstructed Au(111) and clean Cu(111) surfaces is available. Therefore, the possibilities presented by these systems inspired us to study the behavior and the electronic properties, such as work function, of Co nanoislands on the reconstructed Au(111) and clean Cu(111) surfaces.

2. EXPERIMENTAL DETAILS

In-situ experiments were performed in an ultrahigh vacuum (UHV) chamber with a base pressure better than

*Author to whom correspondence should be addressed.

 1533-4880/2010/10/4663/004 doi:10.1166/jnn.2010.1686

1×10^{-10} torr that was equipped with a scanning tunneling microscope (STM). The Au and Cu single crystals with a miscut angle of 0.1° in the (111) direction were cleaned by repeated cycles of ion beam sputtering with 2.5 keV Ar^+ ions and then annealed at 850 K. The Co with a purity of 99.999+% was deposited by evaporation gun onto the reconstructed Au(111) and clean Cu(111) substrates at room temperature, respectively. The flux of Co deposition was about 0.2 ML per minute and the pressure during the deposition was kept below 2×10^{-10} torr. The morphology was directly observed by homebuilt STM operating at room temperature. Tips were electrochemically cut from polycrystalline W wires and used in UHV with no further treatment. The Co coverage is estimated by the average ratio of the area of Co nanoislands to that of the substrate from 10 STM images taken from different regions of 100 nm × 100 nm. However, for Co on Cu(111), it was reported that the Co nanoislands are three cobalt layer deep, with the bilayer height over the surface and the third layer embedded within the Cu surface layer,[17] and accordingly the coverage of Co coverage on Cu(111) surface is corrected. For *Z–V* measurement, the tip trajectory was recorded with an active feedback at a set tunneling current, while the sample bias was ramped from 6 to 9 V, and *Z* is the distance between tip and sample. All *Z–V* experiments were performed at 4 K. The *dZ/dV–V* spectrum was obtained by numerical differentiation of the *Z–V* curve. The experimental details concerning the *dZ/dV–V* spectrum have been described elsewhere.[19]

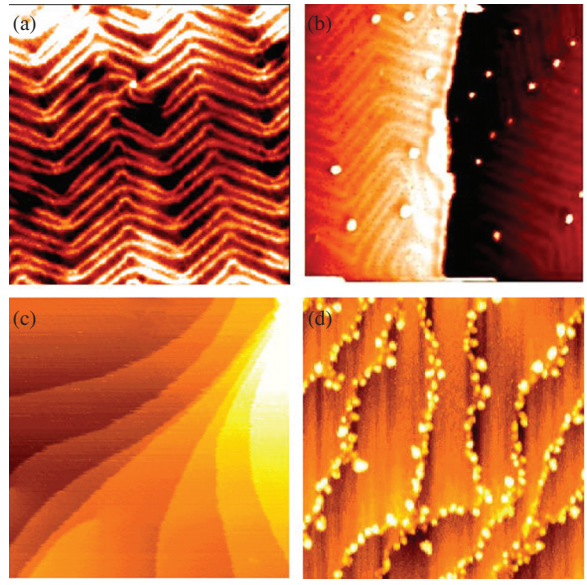

Fig. 1. STM images of (a) clean Au(111) surface (80 nm × 80 nm), (b) 0.005 ML Co deposited on Au(111) surface (70 nm × 70 nm), (c) clean Cu(111) surface (80 nm × 80 nm), and (d) 0.2 ML Co deposited on Cu(111) surface, scanned at room temperature (80 nm × 80 nm).

3. RESULTS AND DISCUSSION

Figure 1(a) shows an STM image of the clean Au(111) surface. The prominent feature of the Au(111) surface is a series of parallel zigzag ridges, the well-known $23 \times \sqrt{3}$ herringbone reconstruction, formed by a stress-induced surface contraction along the line perpendicular to the ridges.[11] Figure 1(b) shows the topographical image of Co deposited on the reconstructed Au(111) surface. Clearly, Co atoms aggregate to the ridges sites and step edges to form Co clusters with an average height of 4.1 ± 0.2 Å (about bilayer height) and average width of 30 Å. This aggregation occurs because the Co atoms have sufficient kinetic energy from thermal energy to migrate to the energetically stable locations, such as the ridges sites and step edges of the reconstructed Au(111) surface.[20]

On the other hand, the clean Cu(111) surface shows atomically flat terrace with average width of about 300 Å separated by the steps with 2.09 Å height as shown in Figure 1(c). Figure 1(d) shows the topographical image of Co deposited on the Cu(111) surface. It is found that almost all cobalt islands are grown at the upper step edge after Co deposition. It might ascribe to an activation barrier of 1 eV existed at the upper edge of Cu steps to prevent the mobile Co adatoms from jumping down the step, and this result is in accordance with the total energy calculations within density functional theory.[21] It is similar to preferential condensation at upper terrace for Fe/Cu(111) system.[22] Besides, the islands have an apparent average height of 3.9 ± 0.2 Å and width of ~48 Å, which corresponds to double-layer patches with respect to lower terrace.

Also, in this study, scanning tunneling spectroscopy (STS) was used to acquire *Z–V* spectra in order to study the electronic properties of Co nanoislands on the Au(111) and Cu(111) surfaces, respectively. If the bias between tip and sample is small, only the image potential state, resulting from its own charge, will be obtained. An electron brought out of the surface will see a positively charged image of itself.[23] Accordingly, we adopted a higher bias from 6 to 9 V to study the transmission behavior of the electron and avoid image potential effect in this study. Figures 2(a) and (b) present *Z–V* curves and *dZ/dV–V* spectra of a Co nanoisland and Au(111) surface, respectively. It is seen that the distance (*Z*) between tip and sample at the setting fixed tunneling current is in stepped increments as the bias *V* increases, as shown in Figure 2(a). This occurs because the triangular potential well forms whenever the fermi level (E_f) of one electrode is greater than the work function of the other. If the bias is increased, the STM retracts to maintain a constant tunneling current and the tip will try to follow the trajectory of the constant electric field. However, whenever the fermi level lines up with the eigenstate of the well, the current tends to increase, causing the STM to withdraw farther.

Another interesting point is that Gundlach oscillation is observed for not only a single Co nanoisland, but also Au(111) surface as shown in Figure 2(b). The origin of

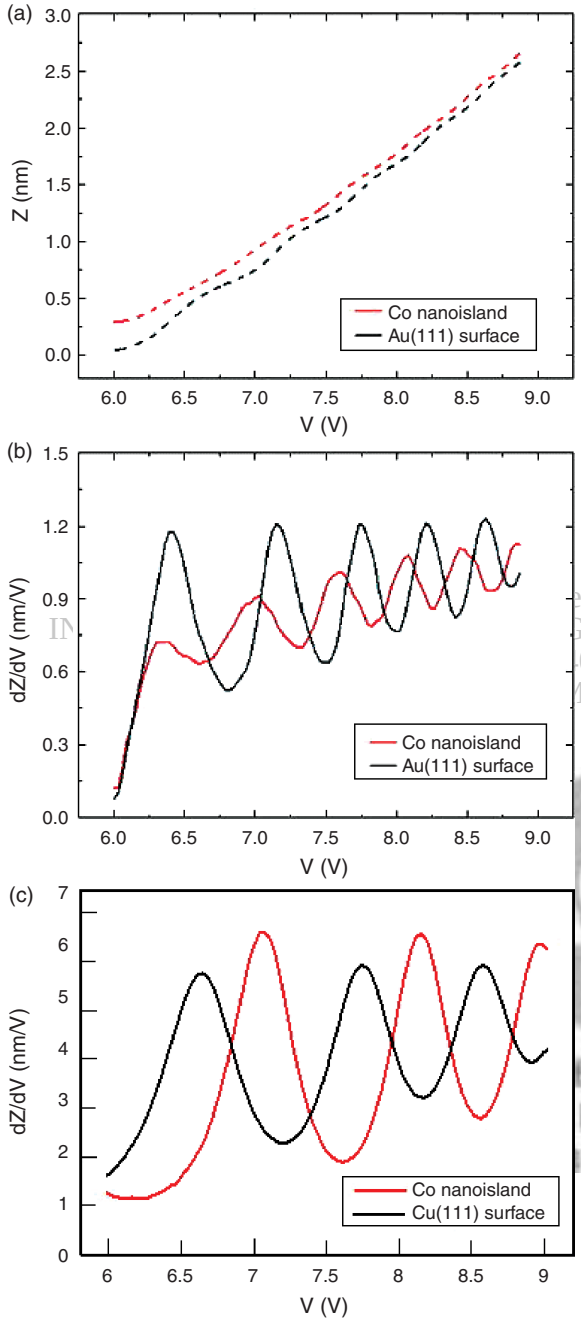

Fig. 2. (a) *Z–V* curves and (b) *dZ/dV–V* spectra of Au(111) and Co nanoisland at the range of 6–9 V in the Co/Au(111) system, and (c) *dZ/dV–V* spectra of Cu(111) and Co nanoisland at the range of 6–9 V in the Co/Cu(111) system.

this oscillation is the wavelike properties of the tunneling electrons. The tunneling gap is on the order of the electron wavelength and the electron waves are coherent. Furthermore, the *dZ/dV–V* spectra between Co island and Au(111) surface exhibits the constant separation, and this energy separation can be estimated to be -0.13 ± 0.01 eV.

In addition to the Co/Au(111) system, one of the most well-known systems is the Co/Cu(111) system. Figure 2(c) shows *dI/dV–V* spectra of Co nanoislands and Cu(111) surface, respectively. Similarly, the Gundlach oscillation is also observed for the Co island and the Cu(111) surface, and the energy separations also remain constant in the spectra, 0.41 ± 0.02 eV for Co/Cu(111).

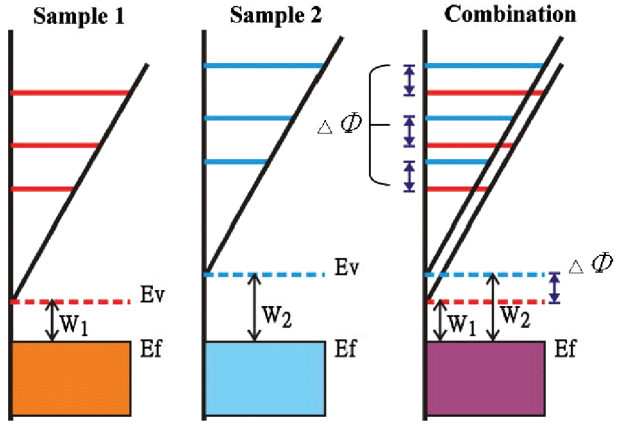

Fig. 3. Schematic for the distribution of standing wave states within a triangular potential. It shows that the energy separation is due to the work function differences between sample 1 and sample 2, i.e., $\Delta\Phi = W_2 - W_1$.

The energy difference in the *dZ/dV–V* spectra between Co island and Au(111) or Cu(111) surface is judged as the difference in the work function between Co island and Au(111) or Cu(111) surface. In general, the work function of a material is defined as the energy which is required to take an electron out of the solid to infinity. Most often it is thought of as a sharp step in the particle's potential energy that occurs at the interface between solid and vacuum. In this study, when the tip is applied with the higher bias than the vacuum level (E_v) of Co adatom or Au(111) surface, i.e., 6–9 V, Gundlach oscillation plays a major role in the spectrum. It is worth noting that with an unchanged electric field the formation of Gundlach oscillation is independent of the characteristics of the observed surfaces, and the distribution of the standing wave states is similar for different materials when they all occur above the vacuum level (E_v).[24] Thus only the beginning of the triangular potential varies with the surface, i.e., the work function. Therefore, during the *Z–V* measurement, the standing wave states of the sample and the substrate can be distinguished due to the difference of work function ($\Delta\Phi = W_2 - W_1$) as shown in Figure 3. In sum, the energy separation measured in Gundlach oscillation should be constant and equivalent to the difference between the substrate and the sample. Through the *Z–V* measurement, it can be understood that even a nanometer scale material can devote itself to the variation of work function for a Co nanoisland on Au(111) or Cu(111) surface.

4. CONCLUSIONS

Co nanoislands aggregate at the upper step edges of the Cu(111) surface and at the step edge and the dislocation sites on the Au(111) surface. Based on *dZ/dV–V*

spectra, both Co/Cu(111) and Co/Au(111) systems exhibit Gundlach oscillation. From the peak shift of *dZ/dV–V* spectra between Co nanoisland and substrate surface, we can quantitatively obtain that the constant energy separation is -0.13 ± 0.01 eV for the Co/Au(111) system, and 0.41 ± 0.02 eV for the Co/Cu(111) system, respectively. These values indicate the work function differences between Co nanoislands and these surfaces. The *Z–V* measurement might allow us to detect the variation of the work function for different magnetic nanostructures.

Acknowledgments: The authors deeply appreciate the financial support from the Nano-Science research grant of Academia Sinica and the National Science Council, Taiwan, under grant no. NSC-95-2112-M-036-002-MY3 and NSC 98-2112-M-029-001-MY3.

References and Notes

1. C. Chappert, K. Le Dang, P. Beauvillain, H. Hardequint, and R. Renard, *Phys. Rev. B* 34, 3192 (**1986**).
2. W. B. Zeper, F. J. A. M. Greindanus, P. F. Carcia, and C. R. Fincher, *J. Appl. Phys.* 65, 4971 (**1989**).
3. J. Ferré G. Penissard, C. Marliére, D. Renard, P. Beauvillain, and J. P. Renard, *Appl. Phys. Lett.* 56, 1588 (**1990**).
4. R. J. Gambino and R. Ruf, *J. Appl. Phys.* 67, 4784 (**1990**).
5. C. Dupas, P. Beauvillain, C. Chappert, J. P. Renard, F. Trigui, P. Veillet, E. Vélu, and D. Renard, *J. Appl. Phys.* 67, 5680 (**1990**).
6. S. S. Parkin, R. Bhadra, and K. P. Roche, *Phys. Rev. Lett.* 66, 2152 (**1991**).
7. S. S. Parkin, R. F. Marks, R. F. C. Farrow, G. R. Harp, Q. H. Lam, and R. J. Savoy, *Phys. Rev. B* 46, 9262 (**1992**).
8. S. S. Parkin, Z. G. Li, and D. J. Smith, *Appl. Phys. Lett.* 58, 2710 (**1991**).
9. T. C. Huang, J. P. Nosieres, V. S. Speriosu, B. A. Gurney, and H. Lefakis, *Appl. Phys. Lett.* 62, 1478 (**1992**).
10. J. Kohlepp, S. Cordes, H. J. Elmers, and U. Gradmann, *J. Magn. Magn. Mater.* 111, 231 (**1992**).
11. B. Voigtländer, G. Meyer, and N. M. Amer, *Phys. Rev. B* 44, 10354 (**1991**).
12. J. Xu, M. A. Howson, B. J. Hickey, D. Greig, E. Kolb, P. Veillet, and N. Wiser, *Phys. Rev. B* 55, 416 (**1997**).
13. S. Padovani, I. Scheurer, and J. P. Bucher, *Phys. Rev. B* 59, 11887 (**1999**).
14. L. Diekhoner, M. A. Schneider, A. N. Baranov, V. S. Stepanyuk, P. Bruno, and K. Kern, *Phys. Rev. Lett.* 90, 236801 (**2003**).
15. M. O. Pedersen, I. A. Bonicke, E. Lagsgaard, I. Stensgaard, A. Ruban, J. K. Norskov, and F. Besenbacher, *Surf. Sci.* 387, 86 (**1997**).
16. Th. Fauster, G. Rangelov, J. Stober, and B. Eisenhut, *Phys. Rev. B* 48, 11361 (**1993**).
17. A. L. Vazquez de Parga, F. J. Garcia-Vidal, and R. Miranda, *Phys. Rev. Lett.* 85, 4365 (**2000**).
18. O. Pietzsch, A. Kubetzka, M. Bode, and R. Wiesendanger, *Phys. Rev. Lett.* 92, 057202 (**2004**).
19. W. B. Su, S. M. Lu, C. L. Lin, H. T. Shih, C. L. Jiang, C. S. Chang, and T. T. Tsong, *Phys. Rev. B* 75, 195406 (**2007**).
20. C. Goyhenex and H. Bulou, *Phys. Rev. B* 63, 235404 (**2001**).
21. Y. Mo, K. Varga, E. Kaxiras, and Z. Zhang, *Phys. Rev. Lett.* 94, 155503 (**2005**).
22. J. Shen, M. Klaua, P. Ohresser, H. Jenniches, J. Barthel, Ch. V. Mohan, and J. Kirschner, *Phys. Rev. B* 56, 11134 (**1997**).
23. J. G. Simmons, *J. Appl. Phys.* 34, 1793 (**1963**).
24. K. H. Gundlach, *Solid-State Electron.* 9, 949 (**1966**).

Received: 20 July 2008. Accepted: 20 January 2009.